Jan. 2011, Volume 5, No.1 (Serial No. 38), pp. 56-67
Journal of Civil Engineering and Architecture, ISSN 1934-7359, USA

Strengthening of RC T-beams with Shear Deficiencies Using GFRP Strips

Kishor Chandra Panda[1], Sriman Kumar Bhattacharyya[2] and Sudhirkumar V. Barai[3]

1. Department of Civil Engineering, ITER, SOA University, Bhubaneswar, Orissa 751030, India

2. Central Building Research Institute, Roorkee, Uttarakhand 247667, India

3. Department of Civil Engineering, IIT, Kharagpur, West Bengal 721302, India

Abstract: The shear performance, modes of failure, and strain analysis of simply supported reinforced concrete (RC) T-beams, externally strengthened in shear using epoxy bonded glass fiber reinforced polymer (GFRP) strips are focused in the present paper. Six RC T-beams of 2.5 m span without shear reinforcement are cast. Three beams are used as control specimens and rest three beams are strengthened in shear with GFRP strips in U-shape, side bonded at 45° and 90° to the longitudinal axis of the beam. All the beams are tested in a Universal Testing Machine. The test results demonstrate the feasibility of using an externally applied, epoxy-bonded GFRP strips to restore or increase the shear strength of RC T-beams. It is also observed that the RC T-beams strengthened by diagonal side strips outperformed those strengthened with vertical side strips.

Key words: Reinforced concrete (RC), glass fiber-reinforced polymer (GFRP), shear strength, T-beams.

1. Introduction

The fiber reinforced polymer (FRP) strips or sheets are an excellent option for use as reinforcing material because of their high strength and stiffness-to-weight ratio, corrosion resistance, durability, non magnetic, non conductive, high resistance to chemical attack as well as ease of its installation. FRP composites have been used in automobile, electronics, and aerospace engineering for several decades, but the application in civil engineering structure as a reinforcing material is relatively recent. FRP composites are applied these days to many structural elements such as beams, columns, retaining walls, domes, tanks, chimneys etc. due to their performance characteristics, and ease of application and low life cycle costs.

The reinforced concrete (RC) beams are strengthened in a variety of ways. FRP wraps covering the whole cross section of a beam, FRP U-jackets covering the two sides and tension face of a beam, FRP plates placed on the two sides of the beam only, and FRP plates placed at the tension face of the beam. A number of important contributions involving the analytical studies of RC beams with externally bonded FRP in shear are available in the literature [1-7]. The experimental studies on RC rectangular beam, strengthened with CFRP strips in shear have been carried out by several researchers [1, 2, 4, 8-10]. Similarly, the experimental studies on RC T-beams, strengthened with CFRP strips have been contributed by Ref. [5], and CFRP and GFRP strips contributed by Ref. [11]. The researchers have shown that the shear strength of reinforced concrete beams may be substantially increased by bonding FRP strips as external shear reinforcement. The studies also demonstrated that the strengthened beams fail in shear in either of the two modes-FRP rupture and debonding of the FRP from the sides, depending on how the beam is strengthened. Available experimental data indicate that almost all beams strengthened by complete FRP wrapping failed due to FRP rupture and beams

Corresponding author: Kishor Chandra Panda, PhD, associate professor, research fields: FRP-concrete composite systemss, rehabilitation and strengthening of structures, concrete structures, FEM application in civil engineering, structures, steel structures. E-mail: kishoriit@gmail.com.

strengthened by U-jacketing also failed in this mode. In contrast, almost all beams strengthened by side bonding, and in some cases, strengthened by U-jacketing, failed due to FRP debonding. The available experimental data also shows the GFRP strips as external strengthening material are very limited both for rectangular and T-beams. Bousselham and Chaallal [12] demonstrated the interaction between the transverse steel reinforcement and the externally applied CFRP in gaining shear capacity. The objective of the present paper is to investigate the shear behavior, modes of failure, GFRP and longitudinal strain analysis of RC T-beams without shear reinforcement and strengthened with GFRP strips in different configurations and orientations.

2. Experimental Investigation

The experimental investigation is carried out on six (6) simply supported RC T-beams without shear reinforcement. Three beams are tested as control beams and the rest three beams are tested as strengthened beams using GFRP strips in U-shape and side bonded at 45° and 90° to the longitudinal axis of the beam.

2.1 Specimen Description

All the T-beams are 2.5 m long having 250 mm flange width and 60 mm thickness, with 100 mm wide and 200 mm deep web and are designed to fail in shear as per IS: 456-2000 [13]. 2 Nos. 20 mm diameter Tor steel bars are used as flexural reinforcement (area 628.31 mm^2) at the bottom, and 4 Nos. 8 mm diameter Tor steel bars are used in one layer at the top. Total six number of stirrups are provided, (2 Nos.) at the support and (1No.) at the loading points to prevent local shear failure. Reinforcement details for beam specimens are as shown in Fig. 1.

The control specimens, not strengthened with GFRP are labeled 0L, whereas specimens strengthened with one layer of GFRP strip are labeled as 1L. The series S0 refers to specimens with no transverse steel reinforcement. Thus, for example, specimen S0-0L-1 is a beam without steel stirrups (S0), without GFRP layer

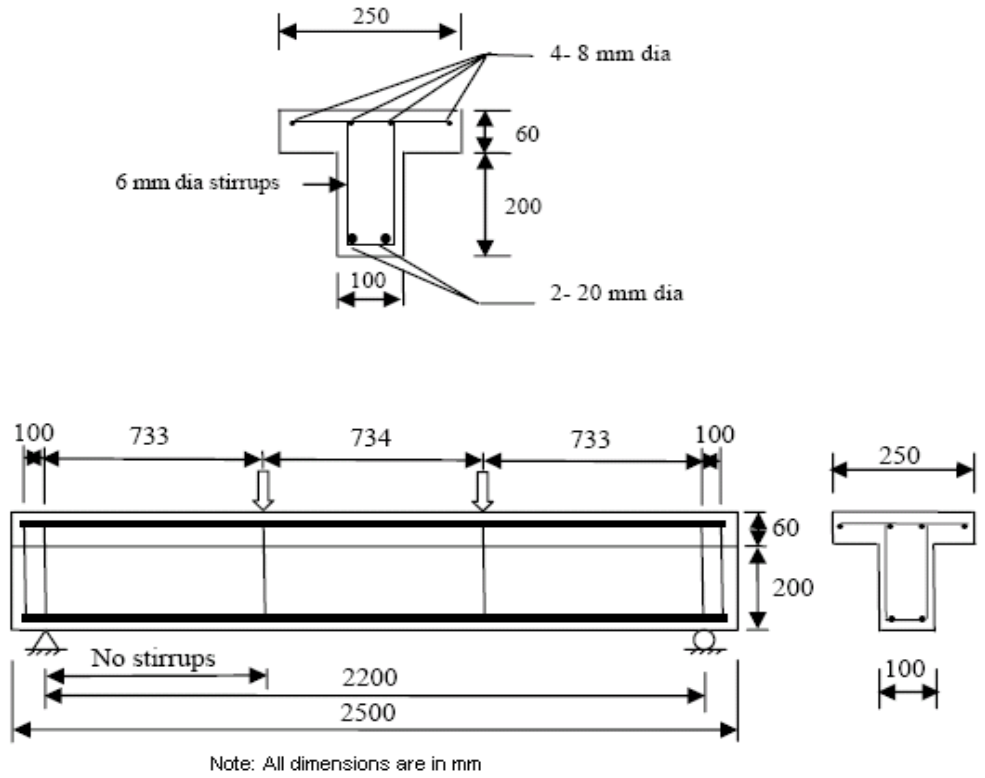

Fig. 1 Reinforcement details for beam specimen.

(0L), and sample number one whereas the strengthened specimen designated as S0-1L-ST-S-45, without steel stirrups, strengthened with one layer (1L) of GFRP strip (ST) on side (S) of the web of the T-beams, and orientation of the fiber angle 90º to the longitudinal axis of the beam. Similarly the specimen S0-1L-ST-S-90 and S0-1L-ST-U-90 is designated.

2.2 Materials and Properties

A concrete mix with Ordinary Portland Cement (OPC- 43 grade) and 12.5 mm down graded coarse aggregates are used for casting. The physical properties of cement and aggregates are presented in Table 1a and Table 1b respectively.

The mix design is carried out for M30 grade of concrete. The mix design proportions of cement, fine aggregate, and coarse aggregate are (1:0.946:2.03). The water cement ratio by weight is 0.375. The slump tests are conducted in each batch of mixing, the value varying between the ranges 30 mm to 50 mm. Compression and split tensile tests on control and strengthened specimen of cubes and cylinders are performed at 7 days and 28 days. The modulus of elasticity is also obtained from the test. The test results of cubes and cylinders are presented in Table 2.

The steel reinforcements used are also tested in the laboratory according to Indian standards. Steels of grade Fe 415 for longitudinal steel reinforcement and Fe 250 for transverse steel reinforcement are used as reinforcement in the experiment. The summary of test results is presented in Table 3.

The width and thickness of the GFRP strip is used for strengthening of RC T-beam is 50 mm and 0.36 mm respectively. Epoxy adhesive is used to attach the GFRP strips to the beam; the resin used is a 9:1 mixture of Araldite CY-230 and hardener HY-951. The spacing between the GFRP strips is 50 mm. The Coupon test is also conducted in a UTM to find out the properties of GFRP strips. The ultimate tensile strength and the elastic modulus measured are 160 MPa and 13.18 GPa respectively.

Table 1a Physical properties of cement.

Characteristics	Value obtained experimentally	Test results supplied by manufacturer	Value specified by IS 8112:1989
Normal consistency (Percent)	31	29	NA
Fineness (m^2/kg)	311	308	225 (min)
Setting time (minutes)			
(a) Initial	130	125	30 (min)
(b) Final	210	220	600 (max)
Specific gravity	3.10	NA	3.15
Compressive strength (MPa)			
(a) 3 days	23.5	37	23 (min)
(b) 7 days	35.54	45	33 (min)
(c) 28 days	49.30	55	43 (min)

Table 1b Physical properties of aggregate.

Characteristics	Value obtained experimentally as per IS: 383-1970	
	Coarse aggregate	Fine aggregate
Type	Crushed	Natural
Maximum size (mm)	12.5 (Angular)	4.75
Specific gravity	2.95	2.64
Total water absorption (percent)	0.53	0.30
Fineness modulus	5.00	2.73 (Grading zone II) Medium sand
Free surface moisture (percent)	Nil	2

Table 2 Test results of cubes and cylinders after 28 days.

Specimen	No. of Beams	Mean compressive strength of cube (MPa)	Mean compressive strength of cylinder (MPa)	Split tensile strength of cylinder (MPa)	Modulus of elasticity as per test results (MPa)
S0-0L	3	49.61	42.16	-	3.465? 0^4
S0-1L-ST-S-90	1	52.18	40.03	2.68	4.264? 0^4
S0-1L-ST-S-45	1	52.18	40.03	2.68	4.264? 0^4
S0-1L-ST-U-90	1	52.18	40.03	2.68	4.264? 0^4

Table 3 Mechanical properties of steel reinforcement used.

Diameter (mm)	Yield stress (MPa)	Ultimate stress (MPa)	Modulus of elasticity (GPa)	Yield strain (μstrains)
20 (Tor steel)	500	590	200	2500
8 (Tor steel)	503	646	180	2794
6 (Mild steel)	252	461	200	-

2.3 Strengthening Configurations

Prior to strengthening, the concrete surface is properly prepared. The small remaining pore spaces are coated with a layer of epoxy based primer, which penetrates in to the concrete pores and provides better bond properties [4]. There is no spalling and delamination on the concrete surface. The corners are grounded to a minimum radius of 10 mm. The bearing substrate surface is roughened by grinding and unevenness in the concrete surface is removed by applying epoxy based mortar. For bonding of GFRP strip, first coat of saturant resin is applied in the GFRP strips marking area followed by the strip. The strip is then coated with a second layer of saturant resin to fully saturate the material and the excessive resin is removed by applying hard roller. The detail preparation stages of strengthened beam are as shown in Fig. 2.

All the T-beams are with the same flexural reinforcement and without transverse reinforcement. One T-beam is strengthened with one layer of GFRP strip in the form of U-shape around the web, and rest two T-beams are strengthened with GFRP strips in 45° and 90° to the longitudinal axis of the beam. The details of the test specimens are listed in Table 4. Where, b_w is the width of the beam cross-section, d is the effective depth of the beam, a/d is the shear span to effective depth ratio, t_f is the thickness of the GFRP sheet, ρ_f is the GFRP shear reinforcement ratio, s_f is the spacing of GFRP strips, ρ_s is the steel web reinforcement ratio, A_{sw} is the total area of transverse steel reinforcement, ρ_w is the longitudinal steel reinforcement ratio, A_{sl} is the total area of longitudinal steel reinforcement, ε_{fu} is the ultimate strain of GFRP strip, ε_{fe} is the effective strain in GFRP strip and E_f is the modulus of elasticity of GFRP strip. The effective strain of GFRP strips is as shown in the Table 4 is the average value of left and right side of the strengthened T-beams.

2.4 Instrumentation and Measurements

All specimens are tested as simple T-beams using two point loading with shear span to effective depth ratio (a/d) equal to 3.26. The tests are carried out at the structural laboratory of Civil Engineering Department, IIT Kharagpur using UTM. Fig. 3 shows the details of the test setup. Five dial gauges are used for each test to monitor vertical displacements. One dial gauge is located at the midspan of the beam. Two dial gauges are located below the loading points and the other two are located at the center of the shear zone on either side of the beam as shown in Fig. 3.

Two types of electrical strain gauges are used in the test; gauges BKNIC-10 (Gauge length is 10 mm, Gauge factor is 2.00 ± 2 %, Resistance in ohms. is 355.0 ± 0.5) are used on the surface of the longitudinal steel reinforcement, and gauges BKCT-30 (Gauge length is 30 mm, Gauge factor is 2.00 ± 2%, Resistance in ohms. 350.5 ± 0.5) are used on the concrete surface.

(a) Cages with strain gauges in longitudinal steel.

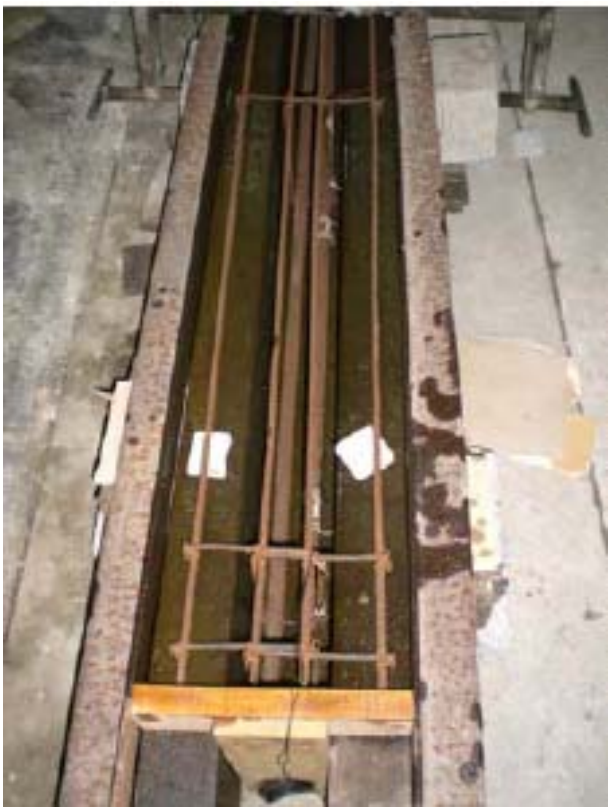

(b) Cages inside mould before casting.

(c) Beam specimen after casting.

(d) Strengthened specimen with GFRP strips.

Fig. 2 Detail preparation stages of the strengthened beams.

Table 4 Details of test specimens.

Specimen	Config.	b_w (mm)	d (mm)	a/d	t_f (mm)	ρ_f (%)	ρ_s (%)	ρ_w (%)	ε_{fu} (10^{-3})	ε_{fe} (10^{-3})	E_f (GPa)
S0-0L	-	100	225	3.26	-	-	0	2.79	-	-	-
S0-1L-ST-S-90	S-90	100	225	3.26	0.36	0.36	0	2.79	12.14	7.293	13.18
S0-1L-ST-S-45	S-45	100	225	3.26	0.36	0.42	0	2.79	12.14	9.604	13.18
S0-1L-ST-U-90	U-90	100	225	3.26	0.36	0.36	0	2.79	12.14	9.229	13.18

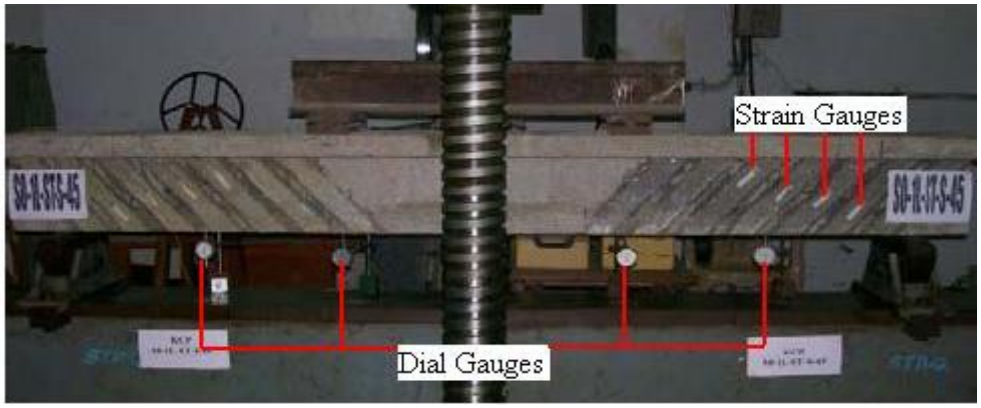

Fig. 3 Details of the test setup with location of dial gauges.

BKNIC-10 is attached on the longitudinal steel to measure deformation during the different stages of loading. In S0-1L-ST-U-90 and S0-1L-ST-S-90 one strain gauge is attached on the longitudinal steel surface at 150 mm distance from the support, whereas in S0-1L-ST-S-45 two strain gauges are used on the longitudinal steel surface at 150 mm and 650 mm distance from the support. The detail location of internal strain gauges is as shown in Fig. 4.

BKCT-30 gauges are attached on the side of the web of the T-beams and to the GFRP surface on the side of the strengthened T-beams and oriented in the GFRP strip direction. Six strain gauges are used on concrete surface, three strain gauges used at the middle of each side of the shear zone as a strain rosette. The location of surface strain gauges on concrete surface is as shown in Fig. 5. Eight strain gauges are mounted on both sides of the strengthened T-beams to the GFRP strip surface on the expected plane of the shear cracks. Four strain gauges are attached on each side as per the cracking pattern of the control beam. The coordinates of strain gauge from left support considering bottom corner as (0, 0) in strengthened beam for Sg1, Sg2, Sg3, and Sg4 are (150, 50), (250, 100), (350, 100), and (450, 150) respectively. Similarly, the same coordinates for Sg5, Sg6, Sg7, and Sg8 are used from right support. The location of surface strain gauges on strengthened beams is shown in Fig. 6.

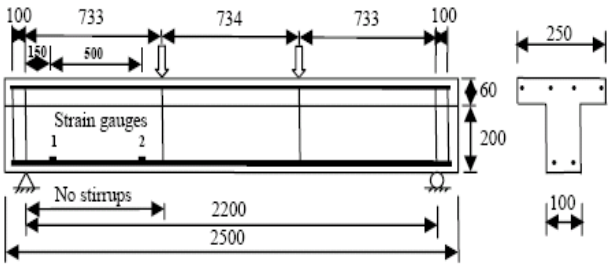

Fig. 4 Location of internal strain gauges.

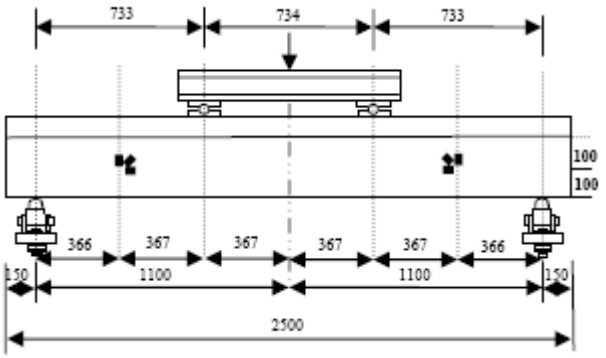

Fig. 5 Location of surface strain gauges on concrete surface.

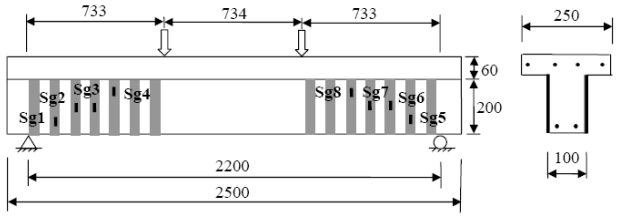

(a) External strain gauges in side bonded GFRP strips with orientation at 90°.

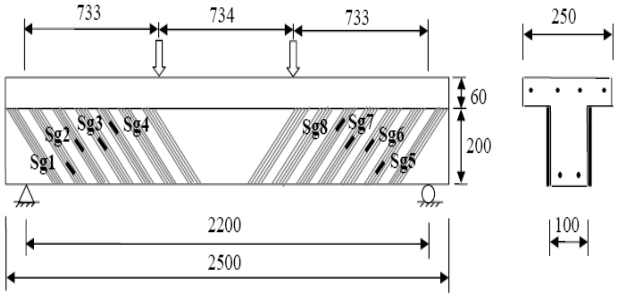

(b) External strain gauges in side bonded GFRP strips with orientation at 45°.

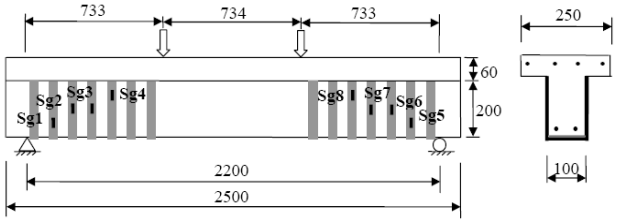

(c) External strain gauges in U-shape GFRP strips with orientation at 90°.

Fig. 6 Location of surface strain gauges on strengthened beam.

3. Results and Discussions

Table 5 shows a comparison between the experimental results of GFRP strengthened RC T-beams and shear resistance calculated based on ACI 440.2R-02 [14] design approach of specimen S0-1L-ST-U-90, S0-1L-ST-S-90, and S0-1L-ST-S-45 and also provides the failure modes observed in the experimental investigation. Fig. 7 shows the experimental results of total applied load versus midspan deflection for the tested beams of U-shape, and side bonded GFRP strips with orientation of the strip at 45° and 90° to the longitudinal axis of the beam.

3.1 Strength

As observed from Table 5, for specimen S0-1L-ST-S-90, the load at ultimate failure attained 116 kN, compared to 100 kN for S0-0L specimen; that is a gain of 16%. As for the influence of the GFRP configuration and orientation on the gain in strength, that is for S0-1L-ST-U-90 and S0-1L-ST-S-45 the loads at ultimate failure are 124 kN and 146 kN respectively. This shows a gain of 24% and 46% respectively on loads over control specimen S0-0L. As expected, without transverse steel reinforcement, the beams strengthened with GFRP side strips perpendicular to the diagonal shear cracks outperformed those strengthened with vertical GFRP strips 90° to the longitudinal axis of the beam and U-jacketed GFRP strips.

3.2 Deflection

As observed from Fig. 7, the midspan deflection of S0-1L-ST-S-90, S0-1L-ST-S-45, and S0-1L-ST-U-90 is 6.98 mm, 10.92 mm, and 8.04 mm corresponding to the load of 116 kN, 146 kN, and 124 kN respectively, whereas in control specimen (S0-0L), the maximum deflection is 6.44 mm corresponding to the load of 100 kN. It may be observed, the midspan deflection in beams, strengthened with GFRP strips is less in comparison to the control specimen for the same amount of load. As expected, the beam strengthened with GFRP strips at 45° orientation to the longitudinal axis of the beam, carry more load and show more deflection than the others.

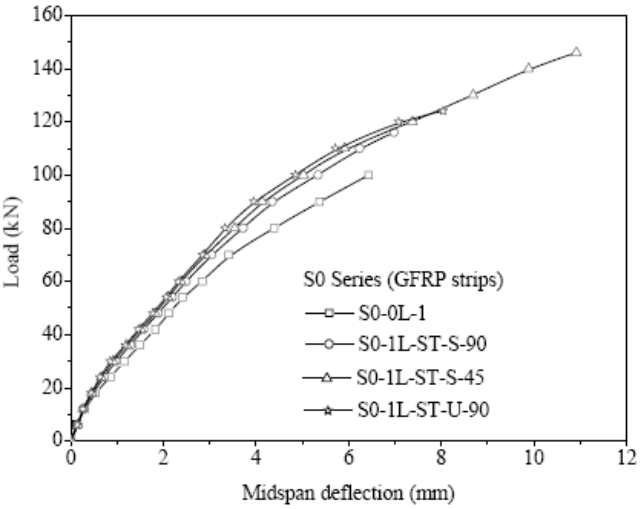

Fig. 7 Load versus midspan deflection.

Table 5 Comparison of experimental and ACI predicted shear resistance results.

Specimen	Experimental results					Theoretical results predicted by ACI 440.2R-02 Design approach			Modes of failure
	Load at failure	$V_{n,test}$	$V_{c,test}$	$V_{f,test}$	$\frac{V_{f,test}}{V_{n,test,rif}} \times$	$V_{f,theor}$	$V_{c,theor}$	$\phi V_{n,theor}$	
	(kN)	(kN)	(kN)	(kN)	100 (%)	(kN)	(kN)	(kN)	
S0-0L	100	50	50	-	-	-	26.68	22.68	Shear compression
S0-1L-ST-S-90	116	58	50	08	16	3.13	26.90	24.44	GFRP debonding
S0-1L-ST-S-45	146	73	50	23	46	5.20	26.90	25.93	GFRP debonding and rupture failure
S0-1L-ST-U-90	124	62	50	12	24	3.13	26.90	24.44	GFRP debonding and rupture failure

3.3 Cracking Pattern and Modes of Failure

The cracking pattern and modes of failure of specimen S0-0L-1, S0-1L-ST-S-90, S0-1L-ST-S-45 and S0-1L-ST-U-90 are as shown in Fig. 8.

Fig. 8(a) exhibits diagonal shear cracks at a load of 70 kN on either side of shear spans of the control specimen S0-0L-1. The cracks started at the center of both shear spans. As the load increases, the crack widened and propagates towards the support and loading points through the flange of the T-beams and leading to failure at a load of 104 kN. At the same time a horizontal crack appeared at the flange and it covers a distance of 275 mm approximately, thereafter, the horizontal crack inclined at approximately 15º angle for a distance of 280 mm. The critical shear crack angle and maximum crack width at the center is approximately 42º and 8 mm respectively at the time of failure.

In specimen S0-1L-ST-S-90, the diagonal shear crack initiated at a load of 70 kN. The crack propagated as the load increases in a similar manner as the specimen S0-0L. The failure occurred due to debonding of GFRP strips over the main diagonal shear crack at a ultimate load of 116 kN as shown in Fig. 8(b). At the same time the diagonal shear crack propagated to the loading position through the flange. In left side of the beam, the strips 2, 3, 4, and 5 debonded from the concrete surface. The debonding length of the strips 4 and 5 is 150 mm and 110 mm from the top of the strip, whereas the strips 2 and 3 debonded from the bottom of the strip for a length of 50 mm and 75 mm respectively. Similarly in right side of the beam, strips 2, 3, and 4 debonded from the concrete surface. The debonding of the strips 3 and 4 is initiated from the top of the strip and is developed for a length of 140 mm and 130 mm respectively, whereas the strip 2 debonded from the bottom for a length of 75 mm. The maximum crack width observed in the web is 3 mm.

In specimen S0-1L-ST-S-45, the GFRP strips are bonded at 45° to the longitudinal axis of the beam. The critical diagonal shear crack initiated at a load of 80 kN in the concrete surface. Thereafter, as load increased, the width of the diagonal shear crack increased slowly, at the same time, the strain in the GFRP strips increased slowly until the load reached the ultimate strength of the control beam. Once the diagonal cracks occurred in the shear span, the strain in the GFRP strip increased rapidly and continued until the beam failed. The ultimate failure of the beam is attained at a load of 146 kN. The failure of the GFRP strips is occured due to GFRP rupture and debonding of the strip from the concrete surface as shown in Fig. 8(c). The failure of the second, third and fourth GFRP strip from the left support is caused by GFRP rupture, whereas the fifth and sixth strip is due to debonding from the concrete surface. The debonding started from the top of the strip. It may be also observed that, the diagonal critical shear crack crosses five GFRP

(a) Shear failure (b) Debonding failure

(c) Debonding and rupture failure of GFRP strips (d) Debonding and rupture failure of GFRP strips

Fig. 8 Cracking patterns and modes of failure.

strips in 45° specimen as compared with 90° specimen, where it crosses four GFRP strips.

It may be observed that, without GFRP strip, in control specimen, the diagonal shear crack appeared approximately in 45° angle, whereas with GFRP strips, the diagonal shear crack observed approximately horizontal as it approaches towards support for a distance of 350 mm.

In S0-1L-ST-U-90 specimen, the critical diagonal shear crack started at a load of 70 kN. As load increased, the width of the crack is also increased, at the same time the strain in the GFRP strip is also increased. Finally the ultimate failure of the beam is attained at a load of 124 kN. The debonding of the GFRP strip is caused from the concrete surface. In left side of the beam, the second GFRP strip is caused by GFRP rupture and debonding as shown in Fig. 8(d), the debonding of the GFRP strip is 160 mm and it developed from the top of the strip, whereas in third strip it developed from the top and debonded the full surface and in fourth and fifth strip it developed from the top and continued for a length of 75 mm and 20 mm respectively. At the ultimate failure, the diagonal shear crack propagated towards loading position through the flange. The crack angle is 44° approximately.

3.4 Strain in GFRP Strips

The curves representing the shear force versus the strains in the GFRP strips for different configuration of series S0 is shown in Fig. 9.

The strain in the GFRP strips in all the strain gauges did not contribute to the shear carrying capacity at the initial stages of loading. In specimen S0-1L-ST-S-90, the strain in the GFRP strip in most of the strain gauges started increasing between 40 kN to 45 kN shear force approximately. Thereafter, as shear force increases, the strain suddenly increases and attained the maximum value of 8884 μstrains at 58 kN shear force. Whereas in specimen S0-1L-ST-S-45 the strain in the GFRP strip

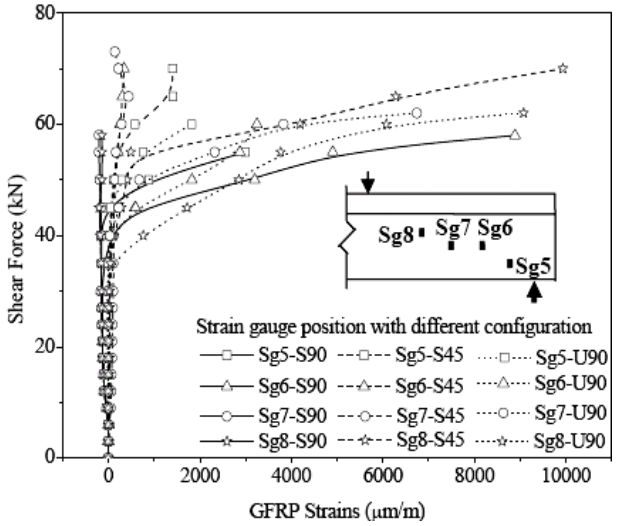

Fig. 9 Variation of strain in GFRP strips for different configurations.

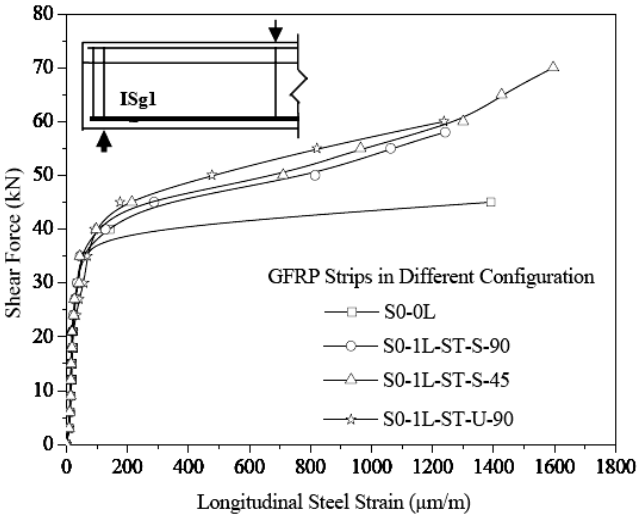

Fig. 10 Variation of strain in longitudinal steel for different configurations.

started increasing in all the strain gauges between 40 kN to 50 kN shear force. The maximum strain observed 9932 μstrains at 70 kN shear force in Sg8 strain gauge. In S0-1L-ST-U-90 specimen, the strain in the GFRP strip started increasing after 35 kN shear force, and attained the maximum value of 9076 μstrains at 62 kN shear force. In series S0, the strain is higher in the specimens strengthened the GFRP strip on side of the web of the T-beams at 45° orientation to the longitudinal axis of the beam, whereas in 90° orientation the strain is less.

3.5 Longitudinal Steel Strain

The curves representing the shear force versus the strains in the longitudinal steel reinforcement for different configuration of GFRP strips of series S0 is shown in Fig. 10.

As observed from Fig. 10, the strain in the longitudinal steel near the support point is very small at the initial stages of loading. As shear force increases, the strain increases linearly up to about 35 kN shear force as the diagonal shear cracks appear in the concrete. After the appearance of diagonal shear cracks in the concrete, the longitudinal steel reinforcement resists the further increments of shear force. In series S0, in control specimen S0-0L, the strain suddenly increases after 35 kN shear force, and attained the maximum value of 1392 μstrains at 45 kN shear force. Whereas in strengthened beam S0-1L-ST-S-90, S0-1L-ST-S-45, and S0-1L-ST-U-90, the strain corresponding to this shear force are 288 μstrains, 215 μstrains, and 176 μstrains respectively. Thereafter, as shear force increases, the strain increases suddenly in strengthened beams and attained the maximum value of 1242 μstrains at 58 kN shear force, 1596 μstrains at 70 kN shear force, and 1238 μstrains at 60 kN shear force in S0-1L-ST-S-90, S0-1L-ST-S-45, and S0-1L-ST-U-90 respectively.

It is observed that, the strain in the longitudinal steel, in beams strengthened with GFRP strips is less as compared with the control beam specimen for the same amount of shear force. It is also observed that, the strain in the longitudinal steel in beam strengthened with U-shape GFRP strips is less as compared to the side bonded GFRP strips for the same amount of shear force.

4. Comparison of Test Results with ACI Prediction

The comparison between the test results and calculated shear strength using the ACI 440.2R-02 [14] design approach is listed in Table 5. $V_{n,test}$= Total nominal shear strength by test, $V_{c,test}$= nominal shear strength provided by concrete obtained from test, $V_{f,test}$

= nominal shear strength provided by GFRP shear reinforcement obtained from test, whereas $V_{n,theor}$ = nominal shear strength calculated theoretically using ACI guidelines, $V_{c,theor}$ = nominal shear strength provided by concrete theoretically, $V_{f,theor}$ = nominal shear strength provided by GFRP shear reinforcement theoretically. It may be observed that the $V_{f,test}$ results are more than the $V_{f,theor}$ results in all the specimens; the ACI design approach gives conservative results for RC T-beams strengthened in shear with GFRP strips.

5. Conclusions

This paper presents the results of an experimental investigation involving six full scale simply supported RC T-beams strengthened in shear with externally bonded GFRP strips, without the transverse steel reinforcement. The test results clearly indicate that for strengthened RC T-beams in shear with side bonded and U-shaped GFRP strips increase the effectiveness by 16% to 46%.

The important conclusions emerging out from this research are as follows:

The gain in shear capacity is significant in all the RC T-beams strengthened in shear with GFRP strips. But so far as the configuration and orientation is concerned, side bonded configuration with orientation of the GFRP strips at 45° to the longitudinal axis of the beam is more effective than side bonded with 90° orientation and U-shape configuration.

The modes of failure of strengthened RC T-beams in shear with side bonded GFRP strips clearly indicate that, the strip at 90° to the longitudinal axis of the beam fails due to GFRP debonding, whereas for 45° orientations and for U-shaped GFRP strip the fails is due to both GFRP rupture and debonding.

The load-deflection graph clearly indicates that the RC T-beams strengthened in shear with GFRP strips have a significant effect on beams ductility. The RC T-beams, becomes more flexible and more deformable, after strengthened by GFRP strips.

The shear force-GFRP strain graph clearly indicates that the strain is higher in the specimens strengthened the GFRP strip on side of the web of the T-beams at 45° orientation to the longitudinal axis of the beam, whereas in 90° orientation the GFRP strain is less.

The GFRP strip does not contribute to the shear carrying capacity at the initial stage of loading still attaining the diagonal shear crack in the concrete.

The strain in longitudinal steel is more strained in control specimens, as compared with strengthened specimens. As far as configuration of GFRP strips is concerned, the U-shape GFRP strips resulted in a decrease of strains in the longitudinal steel reinforcement as compared with side bonded GFRP strips. Also as far as orientation is concerned, the strain in the longitudinal steel at 45° orientation of GFRP strip is less as compared with 90° orientation of GFRP strip.

Acknowledgments

The authors express their sincere gratitude to the structural engineering laboratory, IIT Kharagpur, India, for their technical support and material support for the experimental work. The work presented here is the result of part of the research work.

References

[1] O. Chaallal, M. J. Nollet and D. Perraton, Shear strengthening of RC beams by externally bonded side CFRP strips, J. Compos. Constr. 2 (2) (1998) 111-113.

[2] T. C. Triantafillou, Shear strengthening of reinforced concrete beams using epoxy bonded FRP composites, ACI Struct. J. 95 (2) (1998) 107-115.

[3] T. C. Triantafillou and C. P. Antonopolous, Design of concrete flexural members strengthened in shear with FRP, J. Compos. Constr. 4 (4) (2000) 198-205.

[4] A. Khalifa, W. J. Gold, A. Nanni and A. Aziz, Contribution of externally bonded FRP to shear capacity of RC flexural members, J. Compos. Const. 2 (4) (1998) 195-201.

[5] A. Khalifa and A. Nanni, Improving shear capacity of existing RC T-section beams using CFRP composites, Cement Concr. Compos. 22 (2000) 165-174.

[6] J. F. Chen and J. G. Teng, Shear capacity of FRP-strengthened RC beams: FRP debonding, Constr. Build. Mater. 17 (1) (2003a) 27-41.

[7] J. F. Chen and J. G. Teng, Shear capacity of

fiber-reinforced polymer strengthened RC beams: Fiber reinforced polymer rupture, J. Struct. Eng. 129 (5) (2003b) 615-625.

[8] G. J. Al-Sulaimani, A. Sharif, I. A. Basunbul, M. H. Baluch and B. N. Ghaleb, Shear repair for reinforced concrete by fiberglass plate bonding, ACI Struct. J. 91 (3) (1994) 458-464.

[9] Z. Zhang and C. T. T. Hsu, Shear strengthening of reinforced concrete beams using carbon-fiber-reinforced polymer laminates, J. Compos. Constr. 9 (2) (2005) 158-169.

[10] S. Y. Cao, J. F. Chen, J. G. Teng, Z. Hao and J. Chen, Debonding in RC beams shear strengthened with complete FRP wraps, J. Compos. Constr. 9 (5) (2005) 417-428.

[11] C. Deniaud and J. J. R. Cheng, Shear behavior of reinforced concrete T-beams with externally bonded fiber-reinforced polymer sheets, ACI Struct. J. 98 (3) (2001) 386-394.

[12] A. Bousselham and O. Chaallal, Effect of transverse steel and shear span of the performance of RC beams strengthened in shear with CFRP, Composites: Part B 37 (2006) 37-46.

[13] Indian Standard, Plain and Reinforced Concrete Code of Practice IS 456: 2000, India, 2000, p. 100.

[14] ACI Committee 440, Guide for the Design and Construction of Externally Bonded FRP Systems for Strengthening Concrete Structures (ACI 440.2R-02), American Concrete Institute, Farmington Hills, Michigan, USA, 2002, p. 45.